Formation of low time-bandwidth product, single-sided exponential optical pulses in free-electron laser oscillators

A. M. MacLeod,[1,*] X. Yan,[1] W. A. Gillespie,[1] G. M. H. Knippels,[2] D. Oepts,[2] A. F. G. van der Meer,[2] C. W. Rella,[3] T. I. Smith,[3] and H. A. Schwettman[3]

[1]*School of Science and Engineering, University of Abertay Dundee, Bell Street, Dundee DD1 1HG, United Kingdom*

[2]*FOM-Institute for Plasma Physics ''Rijnhuizen,'' P.O. Box 1207, 3403 BE Nieuwegein, The Netherlands*

[3]*Stanford Picosecond Free-Electron Laser Center, W. W. Hansen Experimental Physics Laboratory, Stanford University, Stanford, California 94305-4085*

(Received 21 April 2000)

The detailed shape of picosecond optical pulses from a free-electron laser (FEL) oscillator has been studied for various cavity detunings. For large values of the cavity detuning the optical pulse develops an exponential leading edge, with a time constant proportional to the applied cavity detuning and the quality factor of the resonator. This behavior has been observed at two separate FELs that have completely different resonator layouts and electron beam characteristics, and using different methods of optical pulse length measurement. The optical pulses have a full width at half maximum time-bandwidth product $\Delta t_{\mathrm{FWHM}} \Delta f_{\mathrm{FWHM}}$ of 0.2–0.3. The results presented here can be used to predict the optical pulse length and corresponding minimum spectral width that can be generated in a FEL pumped by short electron bunches. This is important for the design of new infrared free-electron laser user facilities, which need to make a balanced choice between short pulses for high temporal resolution and narrow bandwidth for linear and nonlinear spectroscopy.

PACS number(s): 41.60.Cr

I. INTRODUCTION

Free-electron lasers (FELs), operating over a large range of wavelengths and optical pulse lengths, have proved to be extremely useful for many experiments, especially in the mid- and far-infrared (3–1000 μm), and several international infrared user facilities have been constructed to exploit this [1]. Although competition from solid-state laser systems, such as Ti:sapphire laser pumped optical parametric generators, is strong at the shorter wavelengths, the FEL has the unique capability of allowing the user to select the appropriate optical pulse duration—or spectral width—for the system under investigation. This feature, combined with the high optical pulse energy, Fourier-transform-limited spectrum, and diffraction-limited beam quality makes the FEL an indispensable tool for linear and nonlinear spectroscopy and experiments requiring high temporal resolution. Recently, variable bandwidth pulses from the FELIX (free-electron laser for infrared experiments, Nieuwegein, the Netherlands) laser were used to systematically characterize the dynamics of the local vibrational modes of hydrogen in CaF_2 [2]. First, a narrow laser bandwidth was used to investigate the dynamics (lifetime and dephasing) of the lowest excited state. Then, by increasing the bandwidth, additional states of the anharmonic ladder were included in the excitation, leading to quantum beating between the multiple excited states. Flexibility in the laser bandwidth enabled a clearer picture of the vibrational dynamics.

Previous characterizations of the optical output of FELs operating in the infrared part of the spectrum have been limited to intensity autocorrelation measurements, with the noticeable exceptions of FROG measurements at Stanford [3], and experiments using a novel Rydberg-atom-based streak camera at (far)-infrared wavelengths [4]. The intensity autocorrelation measurements yield no information on possible asymmetries in the optical pulse, and, indeed, little information about the exact shape of the pulse is obtained: only its duration can be estimated. In this paper we describe results from a series of pulse shape measurements, obtained by cross-correlating the FEL pulse with an ultrashort Ti:sapphire laser pulse. In these experiments detailed information is obtained about the shape of the pulse, and under certain conditions highly asymmetric optical pulses have been observed.

The experiments described in this paper were performed partly on the mid-infrared FEL of the Stanford Picosecond Free-Electron Laser Center [5], and partly on the long wavelength FEL of the FELIX facility [6]. The infrared FEL facilities in both Stanford and the Netherlands were designed to serve an international community of users from a wide range of scientific areas. Although the goals of the two facilities are very similar, there are significant technical differences between the FELs. The laser at Stanford is pumped by an electron beam from a superconducting linear accelerator (linac) and the laser cavity consists of highly reflecting dielectric mirrors, while FELIX uses normal conducting rf linacs and operates with an intra-undulator waveguide and copper mirrors. It is therefore interesting to make a detailed comparison between the optical outputs of the two lasers. A summary of the relevant machine parameters for the two FELs is given in Table I.

Two main optical pulse length measurement techniques were used: differential optical gating measurements [7], and electro-optic cross correlation. In the following sections, the experiments at Stanford and at FELIX are described and the

*Corresponding author. FAX: +44 1382 308688. Email address: a.m.macleod@tay.ac.uk

TABLE I. Overview of the relevant machine parameters for the accelerators and FELs of both the Stanford facility and the FELIX facility used in the experiments described in this paper.

	Stanford mid-IR FEL	FELIX far-IR FEL
	Accelerator parameters	
	Superconducting	Normal conducting
RF frequency (MHz)	1300	3000
Electron bunch frequency (MHz)	11.8	1000
Charge per bunch (pC)	17	200
Bunch length (rms) (ps)	1.0	0.7
Beam energy (MeV)	32	13.1
Normal emittance ($10^{-6}\pi$ rad)	8	70
Energy spread (rms) (%)	0.1	0.2
	Laser parameters	
Wavelength (μm)	6.3	150
Micropulse length (FWHM) (ps)	3–7	1–30
Micropulse energy (μJ)	2	17
Micropulse rep. rate (MHz)	11.8	1000
Macropulse duration (μs)	5000	10
Macropulse rep. rate (Hz)	20	10
Cavity length (m)	12.7	6.0
Cavity round-trip loss (%)	<1	20
Undulator period (mm)	31	65
Number of periods	72	38

experimental data are compared to the results of a one-dimensional (1D) computer model that includes the effects of slippage and short electron bunches [8,9].

II. EXPERIMENTS ON THE STANFORD MID-IR FEL

The experiments at the Stanford facility were performed at a central laser wavelength of 6.3 μm, where the absence of strong atmospheric absorption ensures that there is no temporal distortion of the optical pulse. The cross-correlation measurements of the FEL intensity using a 60 fs Ti:sapphire laser (Tsunami, Spectra Physics, Mountain View, CA) were obtained using the differential optical gating technique to enhance the temporal resolution. The details of the technique are described in Ref. [7]. Here we will limit ourselves to a short description.

A schematic diagram of the experimental setup is shown in Fig. 1. The Ti:sapphire (gate) beam is split into two arms, one of which is delayed with respect to the other by a known amount δ. In both arms the FEL beam and the gate copropagate through a $AgGaS_2$ crystal and the corresponding sum-frequency signals are detected by silicon diodes. The essence of the technique is that, although the FEL and Ti:sapphire gating pulses are imperfectly synchronized (jitter in the system at Stanford has been measured to be of the order of 2 ps [10]), it is possible, by means of an optical delay, to make two closely spaced cross-correlation measurements separated by a time interval—δ in Fig. 1—that is well defined. The precise time at which each such pair of measurements is made is, by definition, uncertain; but each pair can be used to provide accurate estimates of both the average value and the time derivative of the pulse shape at the (unknown) time of measurement. By accumulating, in successive pulses, values of the FEL pulse shape and its derivative at different—and still unknown—times throughout the pulse, a phase-space representation of the pulse is obtained from which its form, as a function of time, can be reconstructed.

The normal FEL resonator at Stanford consists of dielectric mirrors on ZnSe substrates, with a high reflector ($R > 99.5\%$), and an out-coupler ($R = 97.5\%$, 2% out-coupled). For the purpose of this experiment the out-coupler was replaced with another high reflector and measurements were made on the small fraction ($<0.5\%$) out-coupled from it. The reduced losses allow the FEL to operate over a larger range of cavity detunings and allow the formation of longer optical micropulses.

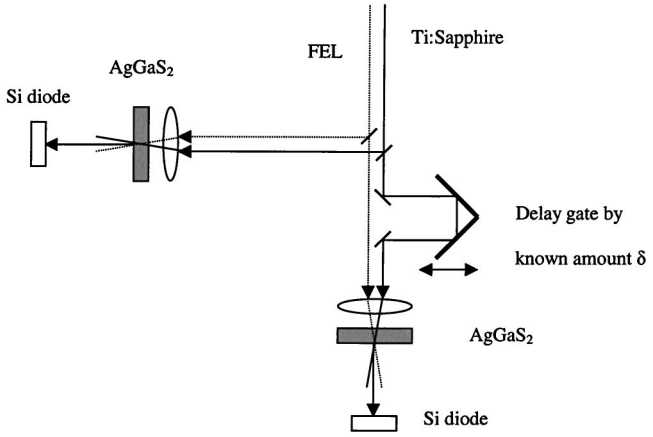

FIG. 1. Schematic of the experimental setup for differential optical gating [7] at a wavelength of 6.3 μm. The Ti:sapphire (gate) beam is split into two arms, one of which is delayed with respect to the other by a known amount δ. In both arms the FEL beam and the gate beam copropagate through a $AgGaS_2$ crystal and the corresponding sum-frequency signals are detected by silicon diodes.

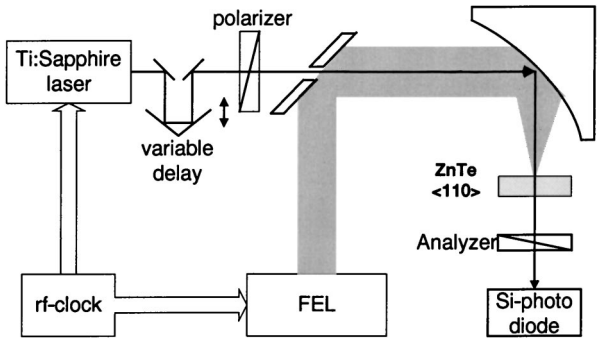

FIG. 2. Schematic of the electro-optic cross-correlation setup. The FEL-induced birefringence in a ZnTe crystal is probed with a synchronized Ti:sapphire laser. A Si photodiode measures the Ti:sapphire intensity passing through a pair of crossed polarizers.

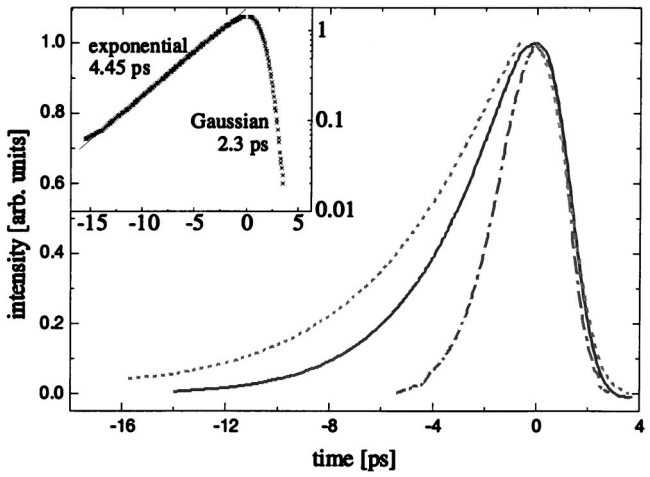

FIG. 3. FEL pulse shape as measured at three different settings of the cavity detuning, -7.65 (dotted line), -4.9 (solid line), and -1.65 μm (dash-dotted line). The inset shows the pulse generated at -7.65 μm in a semilogarithmic format together with a fit to an exponential on the rising edge.

III. EXPERIMENTS AT FELIX

For the experiments performed at FELIX, cross correlation with a 10 fs Ti:sapphire laser (Femto Source Pro HP, Femto Lasers, Vienna, Austria) was used. Pulse shape measurements were performed at a wavelength of 150 μm in the waveguide far-IR FEL by means of electro-optic detection [11] in a ZnTe crystal. Since the jitter between the Ti:sapphire laser and the FELIX FELs is only 400 fs (rms) on a time scale of several minutes [12] and the optical pulse lengths at 150 μm are several picoseconds, the shape of the micropulses could simply be recorded by scanning the delay between the FEL and the Ti:sapphire laser pulse trains. A diagram of the experimental setup is shown in Fig. 2 and the method is described in more detail elsewhere [13]. The optical power spectrum is recorded in the evacuated diagnostic station with a spectrometer equipped with a 48-channel pyroelectric array [14].

IV. DISCUSSION

Figure 3 shows measurements of the optical pulse, taken on the Stanford FEL at a central wavelength of 6.3 μm, and at three different settings of the cavity detuning, $\Delta L = -7.65$ (dotted line), -4.9 (solid line), and -1.65 μm (dash-dotted line). The pulses are clearly asymmetrical and the semilogarithmic plot of the data in the inset (for $\Delta L = -7.65$ μm) shows that the rising edge is an exponential with a time constant of 4.45 ps, while the falling edge is a Gaussian with full width at half maximum (FWHM) of 2.3 ps. Data taken at FELIX, at a wavelength of 150 μm and at detunings $\Delta L = -190$ of (a), -390 (b), and -690 μm (c), shown in Fig. 6 below, show similar exponential rising edges.

The exponential nature of the edge may be understood as follows. This is in fact the *leading* edge of the optical pulse, propagating in a cavity where the losses, characterized by the constant α, reduce the pulse intensity by a factor $e^{-\alpha}$ in each round trip. In a perfectly synchronized FEL cavity, at saturation, the position of the leading edge of the optical pulse remains fixed with respect to the electron bunches at the start of successive round trips. When the FEL cavity is shortened by an amount ΔL, as in the cases described in this paper, the optical pulse moves ahead of the electron bunch by a distance $2\Delta L$ in each round trip. The front part of the optical pulse then decays from round trip to round trip because it has lost contact with the gain medium. In one round trip, the intensity at a point in this part of the pulse is reduced by a factor $e^{-\alpha}$, and in the same round trip the pulse is advanced with respect to the new electron bunch by an amount $\Delta t = 2\Delta L/c$, so that a steady state develops in which the pulse profile in this region shows a time dependence $e^{c\alpha t/2\Delta L}$, i.e., with a time constant of $\tau = 2\Delta L/\alpha c = (2\lambda/\alpha c)\Delta L/\lambda$. This effect was previously noted by Colson [8], although there appears to be a factor of 2 discrepancy with the expression used in this paper.

The data from both FELs exhibit this behavior, as shown in Fig. 4, which shows graphs of the measured value of the leading edge time constant τ against the normalized cavity detuning $\Delta L/\lambda$, together with values calculated from simulations of the micropulse evolution. Simulations were performed using a 1D code [8,9] that, in the case of FELIX only, had been modified to take account of the waveguide in FEL-1. In both cases the simulations used values for the parameter α obtained from independent cavity ring-down measurements. Figure 5, which is typical of a comparison between the measured and simulated pulse shapes for FELIX, shows that the 1D code is able to reproduce the optical pulse shape accurately—in this case at a detuning of -390 μm. The results from Stanford are shown in Fig. 4(a): the experimental data are plotted as solid squares that are seen to follow the expected linear relationship; the results of the simulations are shown as a dashed line; and the least squares fit to the experimental data is shown as a solid line with a slope of $4.4\,\text{ps} \pm 10\%$. The argument presented in the preceding paragraph gives $2\lambda/\alpha c = 4.6$ ps for $\lambda = 6.3$ μm and $\alpha = 0.0091$ (corresponding to a measured cavity $Q \approx 1/\alpha$ of 110). Figure 4(b) presents the FELIX data (solid squares), a best fit line (solid) of slope $4.5\,\text{ps} \pm 6\%$, and the time constants obtained from the simulations (dashed line). In this case $2\lambda/\alpha c = 4.8$ ps for $\lambda = 150$ μm and $\alpha = 0.21$ (obtained from independent measurements of the cavity ring-down time), showing that the optical pulses have again developed an exponential leading edge consistent with the mechanism

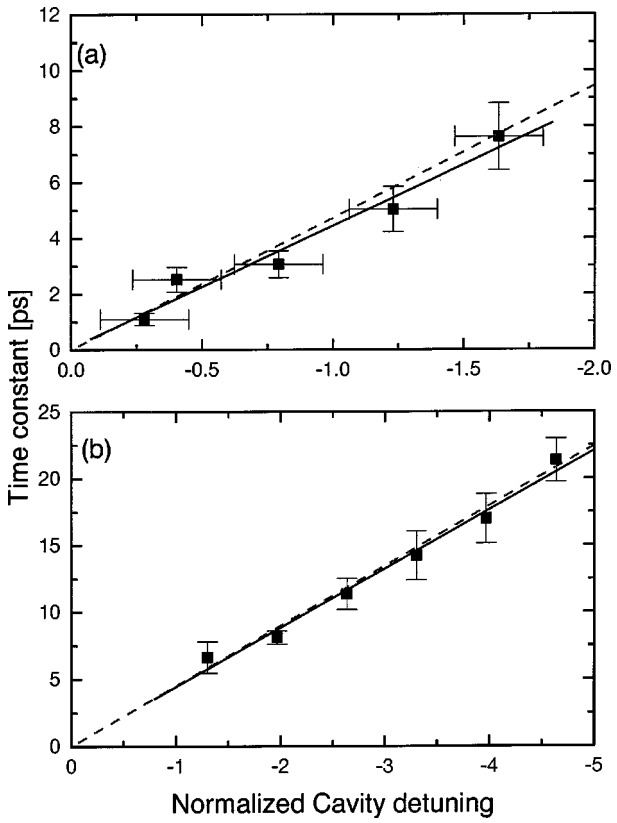

FIG. 4. Measured and simulated exponential time constants of the rising edge of the pulse as function of cavity desynchronism. The data at 6.3 μm from Stanford are shown in (a), while the 150 μm wavelength data taken at FELIX are shown in (b). The solid lines are linear fits to these data; the dashed lines show the results from simulations with a 1D code [8]. See text for details.

described above. It is invariably difficult to determine the exact point of zero detuning; however, this offset may be deduced from the requirement that the graphs of τ against $\Delta L/\lambda$ pass through the origin: the FELIX data required the addition of 0.6λ to the recorded values; no adjustment was made to the Stanford data.

The data from FELIX also include spectral measurements, which illustrate the potential flexibility in selecting pulse and

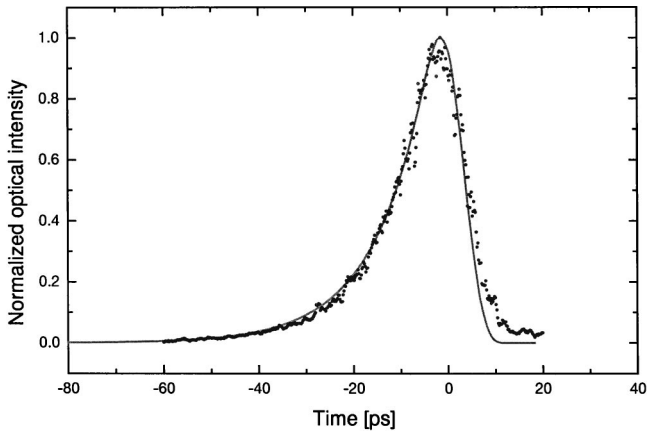

FIG. 5. A comparison of the experimental and simulated optical pulse shapes for FELIX operating at a wavelength of 150 μm and a cavity detuning of -390 μm.

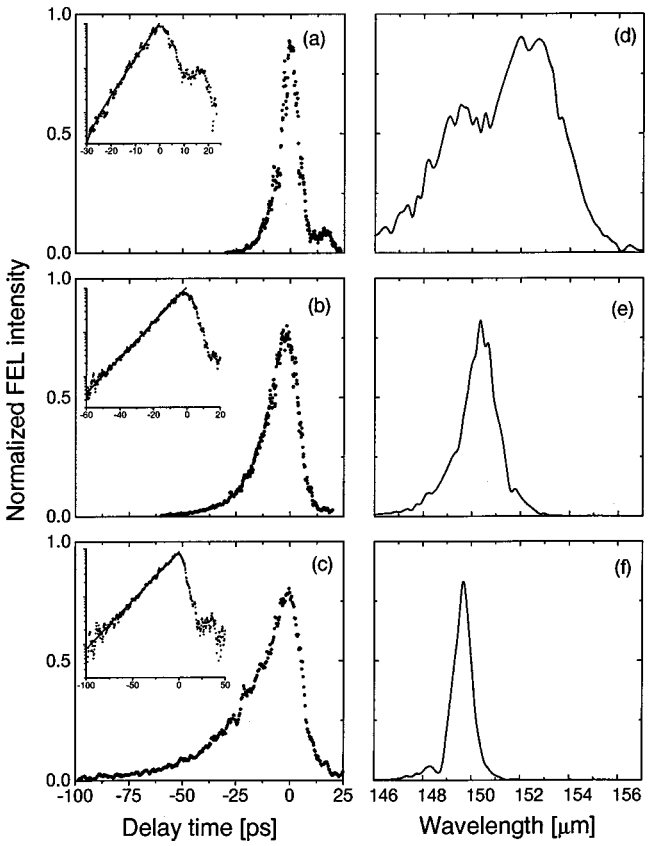

FIG. 6. Measured optical pulse shape (a)–(c) using the electro-optic cross-correlation technique described in the text, and corresponding power spectrum (d)–(f) at a wavelength of 150 μm for different cavity detunings ΔL of (a) -190, (b) -390, and (c) -690 μm. The pulse length is changed from 8.5 (a) to 21 ps FWHM in (c). The solid lines indicate exponential fits to the leading edges.

spectral widths in a FEL by selecting an appropriate cavity detuning. A series of measurements were made at a wavelength of 150 μm and cavity detunings between -190 and -690 μm. Typical results are shown in Fig. 6: pulses in the time domain (a)–(c) with corresponding power spectra (d)–(f) were measured at FELIX operating at a wavelength of 150 μm and at detunings $\Delta L = -190$ μm (c), (d), -390 μm (b), (a) and -690 μm (c), (f). A summary of the results is presented in Fig. 7, which shows that the time-bandwidth product $\Delta t_{\mathrm{FWHM}} \Delta f_{\mathrm{FWHM}}$ remains approximately constant at around 0.2 for normalized cavity detunings in the range -1 to -5, corresponding to pulse durations in the range 2 to 27 ps. This was investigated further by calculating the dependence of the time-bandwidth product of an idealized pulse—with an exponential leading edge and a Gaussian trailing edge, joined at the maximum of the Gaussian—on the time constant of the exponential part. It was found that the value of the time-bandwidth product was relatively insensitive to variations in the width of the Gaussian side over the range of values found in our measurements. The solid curve in Fig. 7 was generated by fixing the Gaussian FWHM at a value of 12 ps and varying the time constant of the exponential over the range found in our experiments. In spite of the crudeness of the model, good qualitative agreement with experiment is obtained. At small detunings, where the exponential edge is very steep, the time-bandwidth product is dominated by the

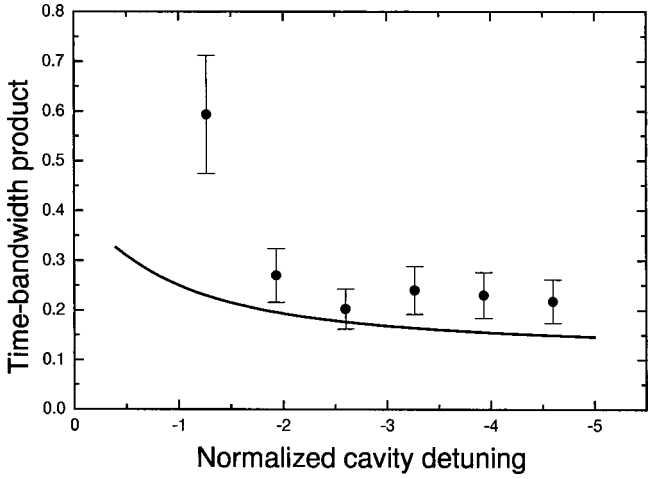

FIG. 7. Time-bandwidth product (FWHM) measured for different cavity detunings (solid dots). The product is in the range 0.2–0.3 if the optical pulse has an exponential leading edge. The product grows to 0.6 for pulses with a more Gaussian pulse shape. The solid line shows the *calculated* time-bandwidth product for pulses with an exponential leading edge and Gaussian trailing edge. See text for details.

Gaussian part (the time-bandwidth product for a Gaussian pulse is $2\ln 2/\pi \approx 0.44$) while for detunings of greater than one wavelength the time-bandwidth product varies slowly, dominated by the effect of the exponential edge and bounded below by the value of $\ln 2/2\pi \approx 0.11$ corresponding to a single-sided exponential.

V. CONCLUSION

It has been shown that optical pulses in two very different FELs, operating in different regimes, evolve an exponential leading edge, and that the time constant for this exponential is proportional to the ratio of cavity detuning to the cavity loss parameter α. A simple model has been presented to explain this effect. It has also been shown that the effect may be adequately modeled by a simple 1D code and that the values obtained from the simulations are in good agreement with experiment both for the Stanford FEL and for FELIX. It has further been shown experimentally that the time-bandwidth product for pulses in a FEL pumped by short electron bunches remains approximately constant over a range of cavity detunings, and indeed that this is in qualitative agreement with calculations made on a simplified pulse shape. This has important consequences for the design of new infrared free-electron laser user facilities that are driven by short electron bunches and that need to make a balanced choice between short pulses for high temporal resolution and narrow bandwidth for linear and nonlinear spectroscopy. Users of existing FELs may use this result to enable them to select the pulse width or spectral width most appropriate to the experiment being undertaken by choosing an appropriate cavity detuning.

ACKNOWLEDGMENTS

This work is part of the research program of the Stichting voor Fundamenteel Onderzoek der Materie (FOM), which is financially supported by the Nederlandse Organisatie voor Wetenschappelijk Onderzoek (NWO). X.Y., A.M.M. and W.A.G. are grateful to the U.K. Engineering and Physical Sciences Research Council for financial support (Contract No. GR/M13602). This work has been supported by ONR Contract No. N00014-94-1024.

[1] G. Ramian, Nucl. Instrum. Methods Phys. Res. A **318**, 225 (1992); R. Prazeres *et al.*, *ibid.* **358**, 212 (1995); F. Ciocci *et al.*, Phys. Rev. Lett. **70**, 928 (1993); K. Imasaki *et al.*, Nucl. Instrum. Methods Phys. Res. A **318**, 235 (1992); W. B. Colson, *ibid.* **429**, 37 (1999).
[2] J-P. R. Wells *et al.*, Phys. Rev. Lett. **84**, 4998 (2000).
[3] R. Trebino *et al.*, Rev. Sci. Instrum. **68**, 3277 (1997); B. A. Richman *et al.*, Opt. Lett. **22**, 721 (1997).
[4] M. Drabbels, G. M. Lankhuijzen, and L. D. Noordam, IEEE J. Quantum Electron. **34**, 2138 (1998).
[5] K. W. Berryman *et al.*, Nucl. Instrum. Methods Phys. Res. A **358**, 300 (1995).
[6] D. Oepts, A. F. G. van der Meer, and P. W. van Amersfoort, Infrared Phys. Technol. **36**, 297 (1995).
[7] C. W. Rella, G. M. H. Knippels, D. V. Palanker, and H. A. Schwettman, Opt. Commun. **157**, 335 (1998).
[8] W. B. Colson, in *Laser Handbook*, edited by W. B. Colson, C. Pellegrini, and A. Renieri (North-Holland, Amsterdam, 1990), Vol. 6, pp. 117–194.
[9] W. B. Colson, Proc. SPIE **1045**, 2 (1989).
[10] R. J. Stanley, R. I. Swent, and T. I. Smith, Opt. Commun. **115**, 87 (1995).
[11] Q. Wu and X. C. Zhang, Appl. Phys. Lett. **71**, 1285 (1997).
[12] G. M. H. Knippels *et al.*, Opt. Lett. **23**, 1754 (1998).
[13] G. M. H. Knippels *et al.*, Phys. Rev. Lett. **83**, 1578 (1999).
[14] G. M. H. Knippels and A. F. G. van der Meer, Nucl. Instrum. Methods Phys. Res. B **144**, 32 (1998).